

Experimental Investigation of the Influence of Metallic Coatings on Yarn Pull-Out Behavior in Kevlar[®] Fabrics

Julie Roark^{1,2}, Frank D. Thomas^{1,2}, Subramani Sockalingam^{1,2,*}, Julia Kempf³, Dan Christy³, Derek Haas³, Daniel J. O'Brien⁴, Kris J. Senecal⁵ and Scott R. Crittenden⁶

¹ McNAIR Aerospace Center, University of South Carolina, Columbia, SC 29201, USA

² Department of Mechanical Engineering, University of South Carolina, Columbia, SC 29208, USA

³ Directed Vapor Technologies International Inc., Charlottesville, VA 22911, USA

⁴ US Army Research Laboratory, Aberdeen Proving Ground, Aberdeen, MD 21005, USA

⁵ US Army DEVCOM-Soldier Center, Natick, MA 01760, USA

⁶ Department of Physics and Astronomy, University of South Carolina, Columbia, SC 29208, USA

* Correspondence: sockalin@cec.sc.edu

Abstract: This work reports yarn pull-out studies of commercially available Kevlar[®] KM2+ individual yarns coated with metallic layers (copper, aluminum, aluminum nitride and silver) via a directed vapor deposition process. The uncoated control and metal-coated Kevlar[®] yarns are hand-woven into fabric swatches for quasi-static pull-out experiments. To perform these experiments, a yarn pull-out fixture is custom-designed and fabricated to apply transverse pre-tension to the fabric. Three levels of transverse pre-tensions are studied at 100 N, 200 N, and 400 N. The results showed that both peak pull-out force and energy absorption during the pull-out process increase with increase in transverse pre-tension. All the metal-coated groups showed an approximately 200% increase in peak pull-out force and a 20% reduction in tenacity compared to uncoated control. Furthermore, all the metal-coated groups showed an increase in energy absorption, with aluminum-coated yarns showing the highest increase of 230% compared to control. These results suggest enhanced frictional interactions during yarn pull-out in metal-coated yarns compared to uncoated control as evidenced by the surface roughness profile of individual fibers and inter-yarn frictional calculations.

Keywords: Kevlar[®]; yarn pull-out; metallic coating



Citation: Roark, J.; Thomas, F.D.; Sockalingam, S.; Kempf, J.; Christy, D.; Haas, D.; O'Brien, D.J.; Senecal, K.J.; Crittenden, S.R. Experimental Investigation of the Influence of Metallic Coatings on Yarn Pull-Out Behavior in Kevlar[®] Fabrics. *Fibers* **2023**, *11*, 7. <https://doi.org/10.3390/fib11010007>

Academic Editor: Catalin R. Picu

Received: 13 November 2022

Revised: 21 December 2022

Accepted: 3 January 2023

Published: 11 January 2023



Copyright: © 2023 by the authors. Licensee MDPI, Basel, Switzerland. This article is an open access article distributed under the terms and conditions of the Creative Commons Attribution (CC BY) license (<https://creativecommons.org/licenses/by/4.0/>).

1. Introduction

Flexible woven textile fabrics utilizing Kevlar[®] fibers are widely used in protective armor applications [1]. During impact, longitudinal and transverse waves develop and propagate in the principal yarns in a fabric that are in direct contact with the projectile [2]. The longitudinal and transverse waves in the primary yarns drive the longitudinal waves in the secondary yarns, thus providing an effective transverse impact on the secondary yarns [3]. This can be understood by considering transverse impact on to a primary yarn, that is, the yarn in direct contact with the projectile. The impact induces longitudinal and transverse waves in the primary yarn resulting in transverse out-of-plane deflection. This transverse deflection drives the orthogonal secondary yarn out-of-plane, providing an effective transverse impact on the secondary yarn. The yarn material behind the longitudinal wave front moves inward towards the impact point resulting in yarn pull-out over the crossover points. Yarn pull-out without premature yarn failure [4] is shown to have a positive correlation to the ballistic impact performance of aramid fabrics [5] due to increased yarn pull-out force and energy dissipation during the pull-out process. Yarn pull-out is influenced by various parameters including inter-yarn friction, pull-out distance, pull-out rate, pull pattern, transverse pre-tension, fiber diameter, fabric architecture, fabric waviness, fabric count and yarn modulus [5–8].

Inter-yarn friction during yarn pull-out is an important energy dissipating mechanism during ballistic impact onto woven fabrics. Increased frictional interactions between the yarns have been shown both experimentally [9] and numerically [10] to improve the ballistic performance of Kevlar[®] fabrics. Previous studies have shown that impact performance can be improved by impregnating fabrics with shear thickening fluid [11], silica nanoparticles [12,13] and carbon nanotubes [9]. A 230% increase in quasi-static yarn pull-out force with tensile strength statistically similar to the neat yarn and a 50% increase in the ballistic limit is reported in [9] for Kevlar[®] 129 fabrics treated with multi-walled carbon nanotubes. In these studies, surface treatments are typically applied to the fabrics rather than to the individual yarns, because weaving of the treated yarns into a fabric may introduce additional damage resulting in tensile strength reduction. However, since the treatment is applied on fabrics, yarn surfaces inside the crossover points may not be as effectively coated. Additionally, in all these studies, a polymer-based surface treatment is typically employed to treat the fabrics, whereas metal-based treatments via vapor deposition techniques for increasing inter-yarn friction are largely unexplored.

The directed vapor deposition (DVD) process [14] can apply well-adhered, inorganic layers onto long lengths of continuous synthetic fibers. The DVD approach provides the technical basis for a flexible, high quality coating process capable of atomistically depositing dense, compositionally controlled coatings onto line-of-sight and non-line-of-sight regions of substrates. Unlike other physical vapor deposition approaches, DVD is specifically designed to enable the transport of vapor atoms from a source to a substrate. To achieve this, DVD technology utilizes a supersonic gas jet to direct and transport a thermally evaporated vapor cloud onto a component. Typical operating pressures are in the 1 to 50 Pa range. In this processing regime, collisions between the vapor atoms and the gas jet creates a mechanism for controlling vapor transport. This enables highly efficient, high-rate deposition (>10 $\mu\text{m}/\text{min}$), non-line-of-sight deposition, and the ability to deposit metals, complex alloys, ceramic layers (including ultra-hard materials) and nano-laminate composites onto complex substrates. The combination of these attributes provides a continuous deposition approach for applying functional layers onto fibers/yarns in a high throughput manner.

While many materials have a higher coefficient of friction than Kevlar[®] (neat Kevlar[®] 129 has a relatively low coefficient of static friction (μ_s) of ~ 0.22 [9]), it is of interest to note that metal-on-metal sliding of simple metals such as Al, Ni, Au, Sn and Cu can have significantly higher μ_s values (μ_s (Al-Al) = 1.0–1.3; μ_s (Cu-Cu) = 1.0; μ_s (Au-Au) = 2.0; μ_s (Ni-Ni) = 0.7–1.1; μ_s (Sn-Sn) = 1.4) [15–18]. It should be noted that these friction values are a function of applied normal force. Of particular interest is the low density of Al that makes thin (nanoscale) layers of well-adhered Al for enhancing ballistic performance via DVD. However, the role of oxidation (which forms on the Al surface in ambient environments) on friction coefficient under various loading conditions is unclear. Other advanced layers also appear feasible via DVD. These include nano-laminates (such as Al/AlN) that may enhance energy dissipation during transverse fiber compression (which can be substantial during impact events) [19–21] through the creation of a high surface area of crack propagation along the multiple Al/AlN interfaces.

In this study, commercially available Kevlar[®] KM2+ individual yarns are coated with metallic layers (copper, aluminum, aluminum nitride and silver) via a directed vapor deposition process. The metal-coated yarns are then hand-woven into fabric swatches. A customized yarn pull-out fixture like the one reported in Zhu et al. [22] is fabricated and is used to investigate the influence of metallic coatings on the quasi-static yarn pull-out behavior. Furthermore, tensile testing is performed to characterize the tenacity, modulus, and failure strain of the yarn for all the coated groups.

2. Materials and Methods

2.1. Manufacturing of Metal-Coated Yarns via Direct Vapor Deposition

Metal-coated Kevlar[®] yarns are created in this work by applying continuous metal films via a gas jet assisted vapor deposition technique. This approach, shown schematically in Figure 1, termed Directed Vapor Deposition (DVD), is based on electron beam evaporation in the presence of an inert carrier gas (see reference [14] for details). Using the DVD process, metallic layers (copper, aluminum, aluminum nitride and silver) are applied onto continuous lengths of 600 denier Kevlar[®] KM2+ yarns. Prior to coating, a hot water scour is conducted to remove the sizing from the As-received yarns. The yarns are scoured using a package dyeing process. The machine was filled at 49 °C and heated to 71 °C for 20 min, then drain and rinse step of 5 min at 49 °C. For moisture removal, drying is performed in a vacuum drying oven with “non-humid” air at 105 °C for 161 min. In package dyeing, the yarn is wound on a small, perforated spool. The winding parameters are set to promote a looser and a more open yarn configuration than typical. The spools are placed into the dyeing machine in which the flow of the dye bath alternates from the center to the outside, and then from the outside to the center of the package. This process infiltrates the entire length of yarn on the spool with the dye. The fluid temperature and the pressure drive the flow of the dye bath and can be adjusted to control the infiltration process.

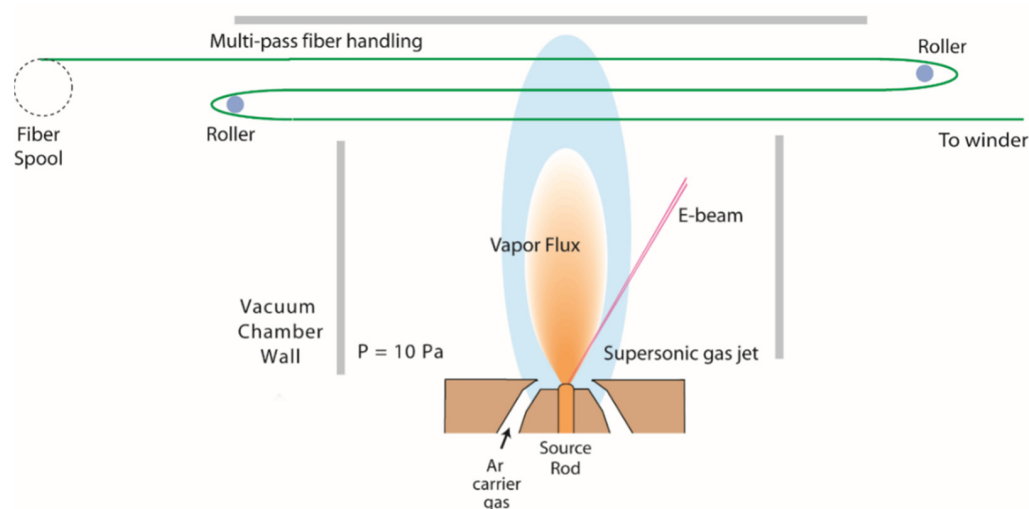


Figure 1. Schematic illustration of the Directed Vapor Deposition (DVD) system having a multi-pass yarn handling system.

The yarns are fed into and out of the deposition zone with a roll-to-roll yarn handling system. This system allows the yarns to pass through the deposition zone multiple times at a chosen line speed (up to 91.44 m/min). The coating material is evaporated using an electron beam gun and entrained in an Argon carrier gas. A chamber pressure of 10 Pa is used during deposition. The resulting layers are hypothesized to modify the friction coefficient of the yarn. Denier measurements (see Table 1) of the yarn are made by cutting a 1-m-long section of the yarn and measuring the mass in a balance with 0.1 mg resolution. A marginal increase in the denier is measured for the coated groups with a maximum increase of 7.6% for the silver coating. The resulting metal-coated yarns are then hand-woven into fabrics using an aluminum loom with stainless steel pins to enable high density of warp yarn ends and provide reduced damage during weaving. The weft is about 33 feet long and the distance between the first and last warp pins was about 3.7" resulting in about 108 passes. The purpose of hand weaving is to screen the type of coating for ballistic impact testing by assessing/ranking the pull-out response of different metal-coated yarns in a less-time consuming and inexpensive way before weaving them via textile weavers. Test fabric swatches are created consisting of 34 warp yarns and ~50 weft yarns with nominal dimensions of 101.6 mm × 25.4 mm as shown in Figure 2.

Table 1. Coated and uncoated experimental groups.

Experimental Group	Description	Linear Density (Denier)	Effective Fiber Diameter (μm)
Control	Hot water rinsed 600 denier Kevlar KM2+	600	12.0
Aluminum	Aluminum Coating on Control	605	12.05
Copper	Copper Coating on Control	637	12.36
Silver	Silver Coating on Control	646	12.45
Aluminum/Aluminum Nitride	Aluminum/Aluminum Nitride Coating on Control	627	12.27
Hybrid Al/Control	Hybrid Aluminum (warp)/Control (weft)	604	12.04
As-received	600 denier KM2+ 34 \times 34 Scoured Fabric Roll	600	12.0

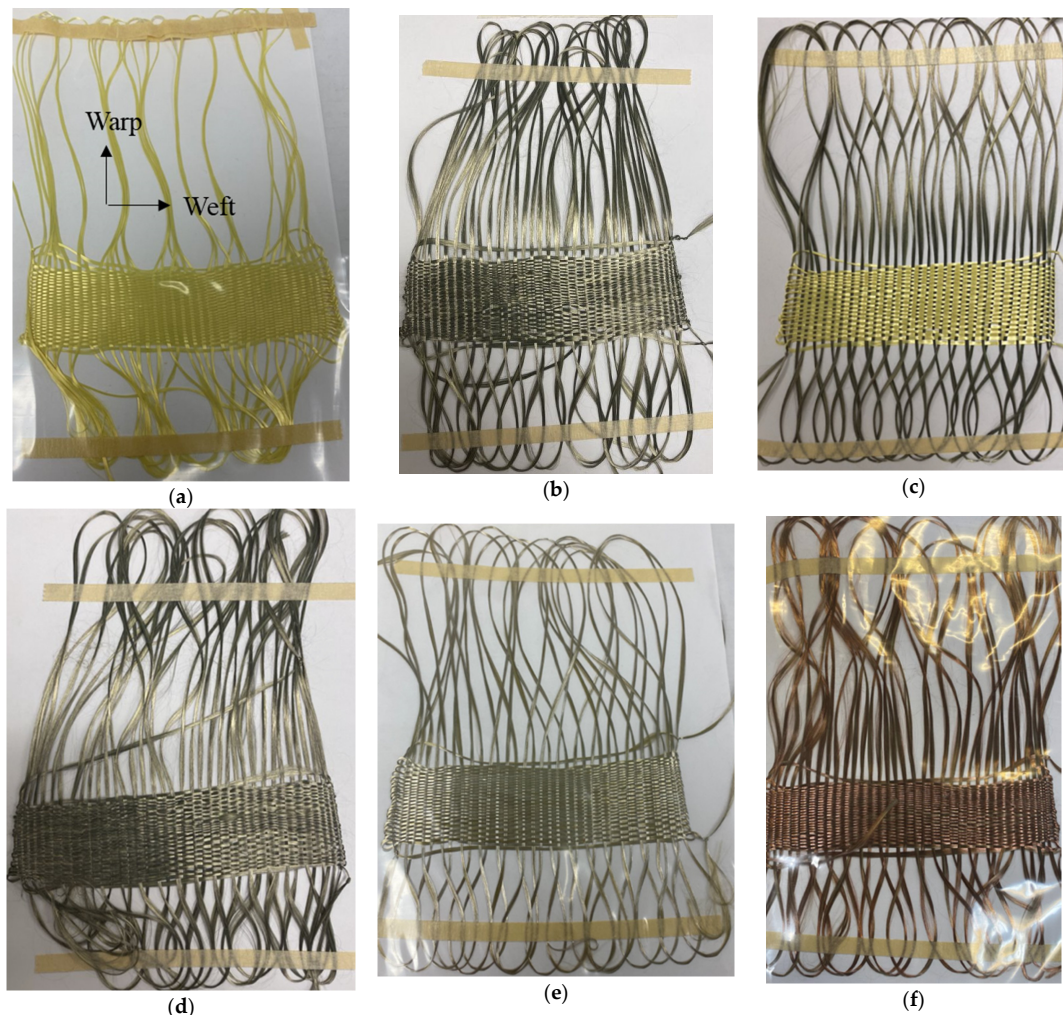
**Figure 2.** Hand-woven fabric swatches (a) Control (b) Aluminum (c) Hybrid Al/Control (d) Aluminum/Aluminum Nitride (e) Silver (f) Copper.

Table 1 shows the various coated groups studied in this work. The “Control” material is 180 g/m^2 , 600 denier sized Kevlar[®] KM2+ yarn rinsed with hot water. “As-received” is the Kevlar[®] S706 scoured plain-woven fabric with 600 denier KM2+ yarns, with a fabric count of 34 \times 34 yarns per inch in warp and weft directions. Each yarn consists of 400 fibers with a nominal diameter of $12.0 \mu\text{m}$. As shown in Figure 2, the coated groups include coatings

of Aluminum, Copper, Silver, Aluminum/Aluminum Nitride, and a Hybrid Aluminum (warp)/Control (weft). The effective fiber diameter is calculated based on the measured denier and the number of fibers (400). In the Hybrid specimen, warp yarns are Aluminum coated whereas the weft yarns are uncoated as shown in Figure 2c. It should be noted that the hand-woven specimens are not as tightly woven compared to the As-received S706 fabric.

Infiltration of metal coating within the fibers in a yarn depends on the process conditions such as pass count, line tension, coating time, and spreading techniques. In this study, an 8-pass ceramic roller is used to improve coating infiltration. Visual examination of fabric and yarn surfaces in Figures 2 and 3a,b shows that the metallic coatings adhere to the Kevlar[®] yarns. Furthermore, scanning electron microscopy (SEM) of individual single fibers extracted from Control and some metal-coated groups are shown in Figure 3. These images confirm the presence of coated material on the fiber surface. As shown in Figure 3d–f, in Al- and Cu-coated fibers, a “bulk” metal layer is observed, whereas in Al/AlN-coated fiber, a distribution of metal particle deposition is observed. Coating quality is complex and difficult to quantify, so further study of infiltration, while important, is beyond the scope of this paper.

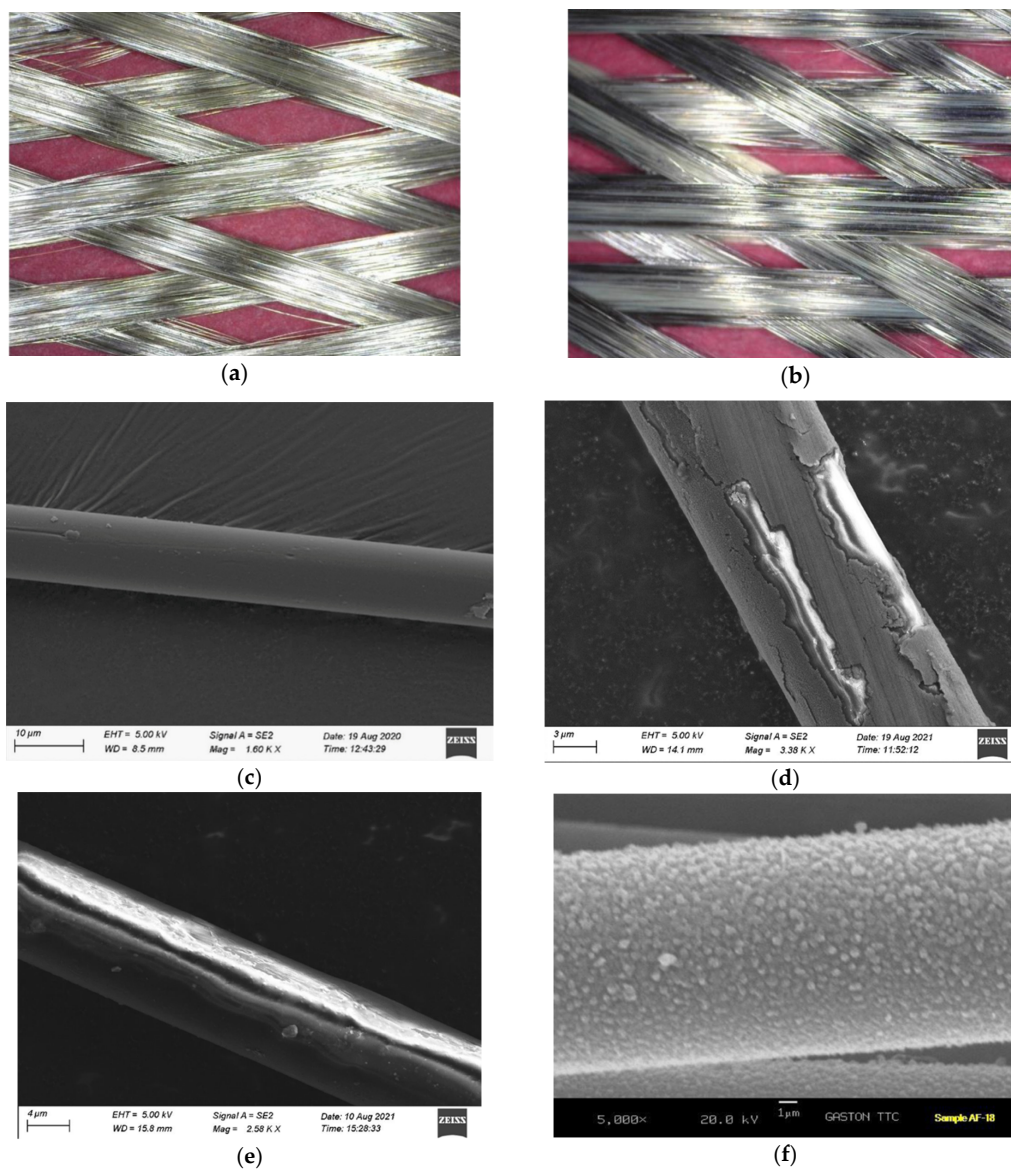


Figure 3. (a) Silver-coated yarn (b) Aluminum-coated yarn; SEM images of single fibers (c) Control (d) Aluminum-coated (e) Copper-coated (f) Al/AlN-coated.

2.2. Quasi-Static Yarn Pull-Out Setup and Test Methodology

The quasi-static yarn pull-out experimental setup developed in this study utilizing an Instron 5944 machine is shown in Figure 4. A custom-designed pull-out fixture is fabricated using Aluminum 6061. The setup consists of a fixed clamp and a sliding/adjustable clamp with a knurling pattern to clamp the fabric specimen with minimum slippage. The sliding clamp can travel along the railing with carriages and is connected to a screw rod with an adjustable knob to apply various transverse pre-tensions (pre-loads) to the specimen. An Interface SML-450N load cell is used to measure the applied pre-tension. As shown in Figure 4, the frame is fixed to the base plate with an X-direction stage to align the yarn to be pulled with the line of action of the Instron's crosshead. A wedge grip attached to a 2 kN load cell is used to pull a single yarn.

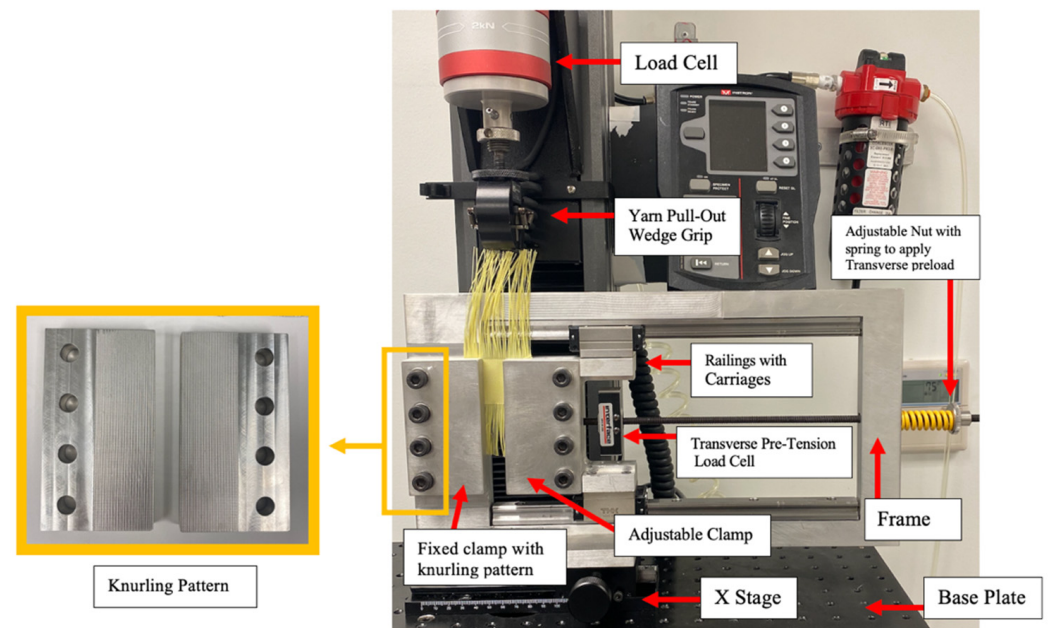


Figure 4. Quasi-static yarn pull-out test setup in an Instron machine.

Figure 5a shows the yarn pull-out specimen with nominal dimensions and the pull pattern used. A nominal fabric length of 32 mm and a tail length of 20 mm is used in all experiments. Pull-out tests are performed on a single fabric specimen at three levels (400 N, 200 N, and 100 N) of transverse pre-tension using a pull pattern sequence of 1001001001001001 as shown in Figure 5a. These load levels are selected based on the literature [22] and our numerical simulations of ballistic impact onto single layer Kevlar[®] S706 fabric. Here, “1” represents a yarn that is being pulled and “0” represents the adjacent yarn that is skipped. A total of 6 pull-out tests are performed on a single fabric specimen such that 2 tests at each of the three transverse pre-tensions in the order of 400 N, 200 N, and 100 N as shown in Figure 5a. 1001001 pull pattern is determined based on the repeatability of results after testing multiple pull patterns of different variations. A displacement rate of 1 mm/s is used for all yarn pull-out experiments. Pull-out force, crosshead pull-out displacement, and transverse pre-tension is recorded. In all experiments, single warp yarns are pulled in the fabric specimens. A relaxation test is performed to confirm there is no slippage present in the fabric clamps that provide transverse pre-tension to the fabric during pull-out experiments. For the relaxation test, a maximum initial transverse pre-tension of 400 N is applied to the specimen and the transverse load decay is monitored for 120 min. As shown in Figure 5b, the load drop is less than 1.30% of the original force applied indicating minimum slippage.

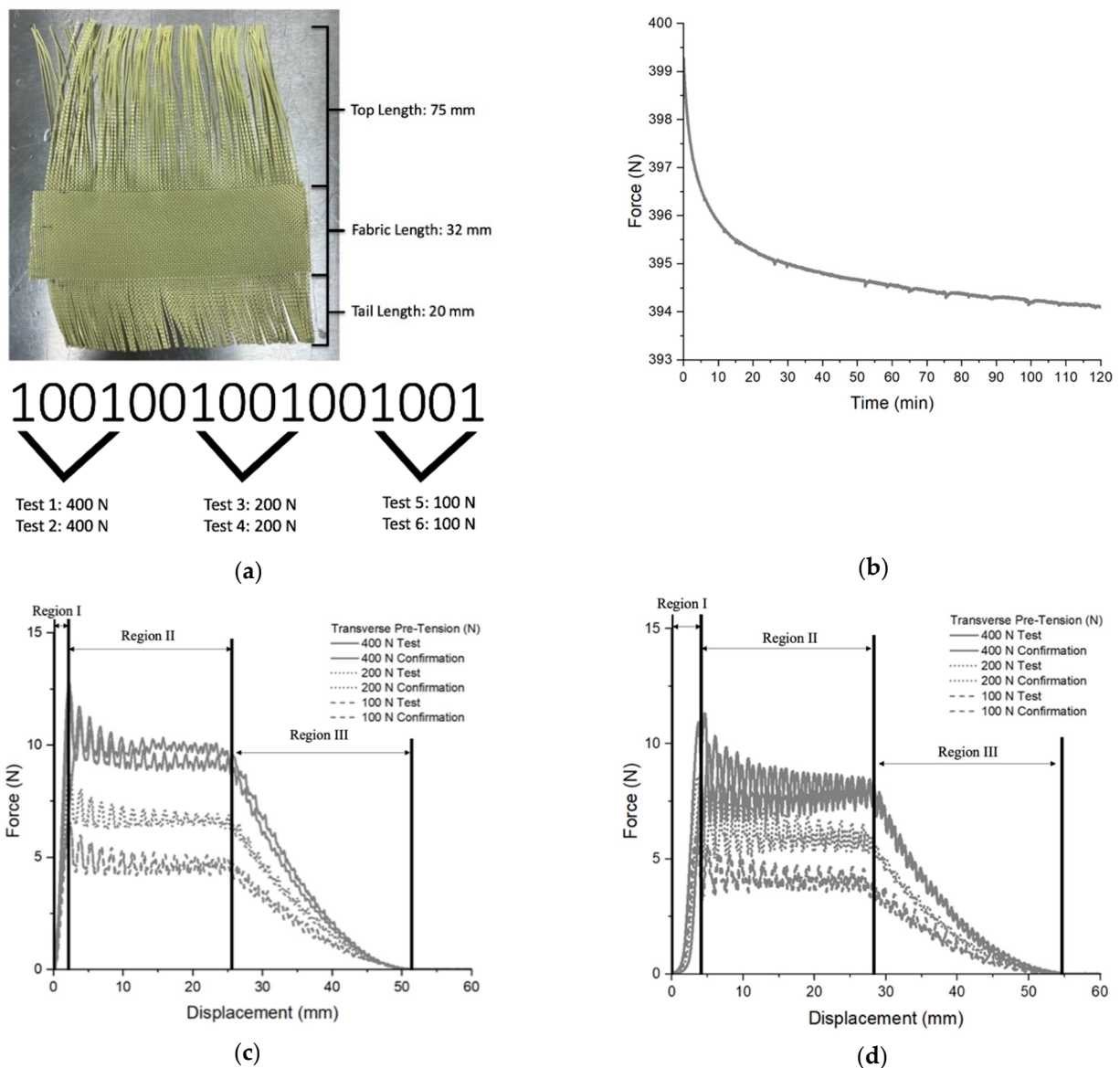


Figure 5. (a) Yarn pull-out fabric specimen (b) relaxation response; pull-out force–displacement response of As-received Kevlar[®] S706 fabric with 600 denier KM2+ yarn (c) weft direction (d) warp direction.

Preliminary yarn pull-out testing using the As-received Kevlar[®] S706 fabric is conducted to ensure the experimental results are reproducible and accurate. As shown in Figure 5c,d, the yarn pull-out load–displacement response is generally comparable to the results published in the literature [6,23] and is repeatable at different transverse pre-tensions. The pull-out response can be described over three distinct regions. In Region I, the pull-out force increases linearly as the yarn being pulled undergoes uncrimping and straightening resisted by the static friction of orthogonal yarns in the woven fabric. The end of Region I is characterized by the peak force associated with static friction. Upon reaching the peak force, that is, overcoming the static friction, the pulled yarn begins to slide with a sudden drop in force observed at the beginning of Region II. The oscillations in Region II are due to the stick-slip behavior as the pulled yarn passes through the orthogonal yarns. The length of Region II is approximately equal to the tail length of the specimen. Finally, in Region III, force decreases to zero as the tail length of the yarn traverses through the fabric and gets completely pulled out. The length of Region III is approximately equal to the length of the fabric.

The integration of pull-out force versus displacement response is used to determine the energy absorbed during the pull-out process for each experimental test. Energy absorption values are divided by the measured tail length and fabric length of each specimen, to allow for consistent results due to the variations in dimensions of the hand-woven specimens.

2.3. Quasi-Static Yarn Tensile Test Setup

Yarns of 254 mm gage length (L_0) from all the experimental groups shown in Table 1 are pulled in quasi-static tension consistent with the ASTM standard D7269-07 [24]. All experiments are performed on an Instron single column tester, Model 5944. A 2 kN load cell and a rate of 127 mm/min is used to test all yarns. Pneumatic Instron grips are used to grip the specimen as shown in Figure 6. For each experimental group, a minimum of 25 specimens are tested.



Figure 6. Yarn tensile testing experimental setup.

The force–displacement measurements from the tensile tests are used to calculate the tenacity versus strain curves using Equation (1):

$$T = \frac{F}{\lambda} \quad \varepsilon = \frac{\Delta L}{L_0} \quad (1)$$

where T is the tenacity, F is the force, and λ is the linear density in denier (see Table 1); ε is strain, L_0 is the original gage length, and ΔL is the change in length.

3. Results

3.1. Yarn Pull-Out Response of Hand-Woven Specimens

Figure 7 compares the pull-out response of As-received Kevlar[®] S706 fabric and the hand-woven Control fabric at 200 N transverse pre-tension. The general response of the hand-woven specimen is similar to the As-received Kevlar[®] S706 fabric with three distinct regions (see also Figure 5c). However, the stick-slip oscillation behavior in Region II is less pronounced, likely due to the “looseness” of the hand-woven weave compared to the As-received S706 fabric. The tightness of the weave in the As-received S706 fabric creates tension in the yarns that result in region II to be more prominent than the hand-woven

fabric. It is observed that the magnitude of peak pull-out force in hand-woven Control is approximately four times lower than the peak force measured in As-received fabric.

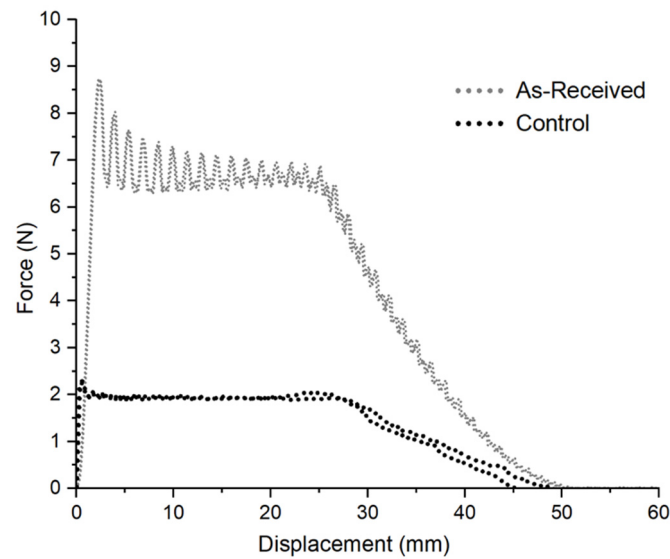


Figure 7. Yarn pull-out force–displacement response of Control and As-received S706 fabrics at 200 N transverse pre-tension.

Figure 8 shows the images of the As-received and hand-woven specimens during the pull-out process at a transverse pre-load of 400 N. Specifically, Figure 8 shows the images before yarn sliding, during yarn sliding, and complete yarn pull-out for As-received, Control, Aluminum/Aluminum Nitride, and Hybrid Al/Control groups. The pull-out process is generally similar for all the metal-coated fabrics. As the yarn pull-out test is initiated, the yarn undergoes an uncrimping process (Region I). The uncrimping process is defined as the straightening of the yarn inside the woven fabric. After the yarn is fully uncrimped, it undergoes translation/sliding until it is completely pulled out from the fabric. The transverse pre-tension applied on the fabric increases the force needed to uncrimp and begin the pull-out process. A high-pitched noise is observed for the metal-coated fabrics during yarn sliding which is not present for Control, Hybrid or As-received samples, thought to be due to the metal-on-metal contact.

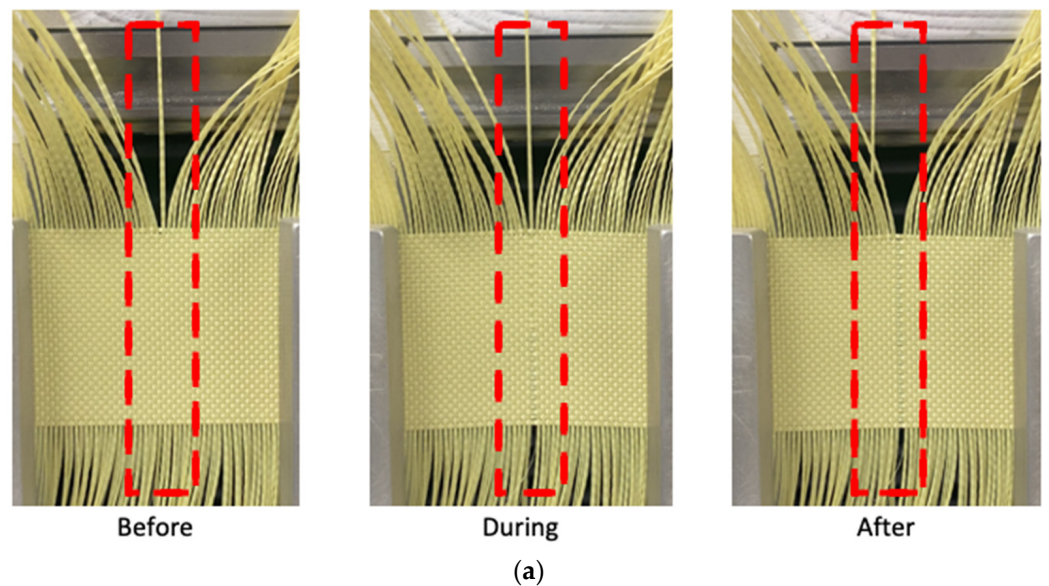


Figure 8. Cont.

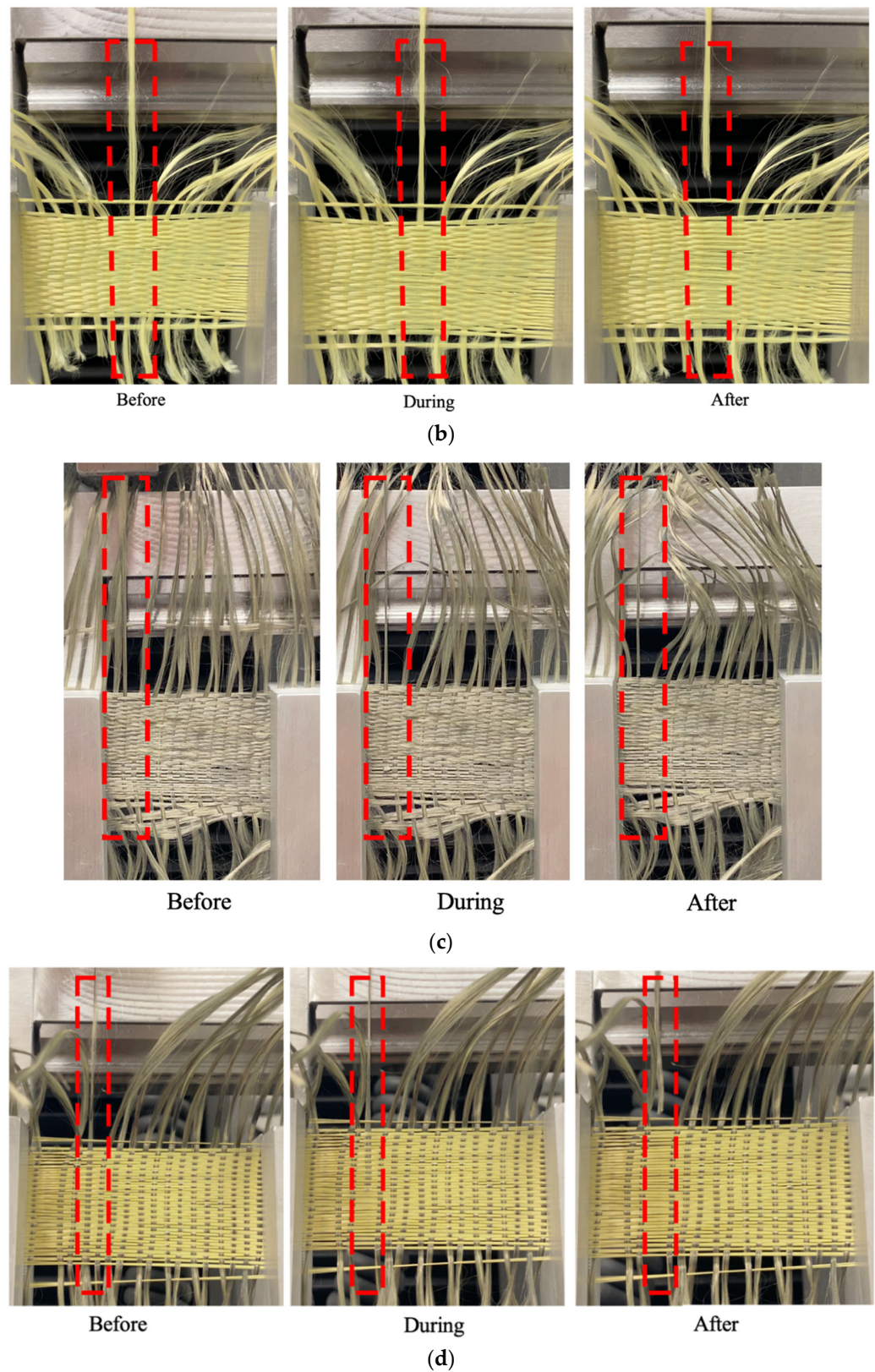


Figure 8. Pull-out process at 400 N transverse pre-tension with pulled yarn highlighted in a box (a) As-received (b) Control (c) AI/AIN (d) Hybrid AI/Control.

Figure 9 shows the yarn pull-out force–displacement response of hand-woven control and metal-coated specimens along with their measured tail length and woven length. The

general response of all the hand-woven specimens are similar to the As-received Kevlar[®] S706 fabric with three distinct regions (see also Figure 5c). The peak pull-out force in Region I is observed to increase with transverse pre-tension for all the groups (quantified later). This is likely due to an increase in the normal force between the orthogonal yarns, which also increases the frictional resistance to yarn pull-out [22]. All the metal-coated groups exhibit a higher peak pull-out force compared to the control at all the transverse pre-tensions studied. As shown in Figure 9a, for control, upon reaching the peak force, the force drop is sudden but minimal, with the force in Region II (yarn sliding) approximately constant at all the transverse pre-tensions studied. However, for the metal-coated groups, the force drop is more gradual and the force in Region II is approximately constant at 100 N and 200 N transverse pre-tensions (Figure 9b–f). At 400 N pre-tension, the force in Region II continuously decreases with displacement. This suggests that yarn sliding/translation occurs non-uniformly in metal-coated specimens, which could be due to the coating being scraped off, compared to a more uniform yarn sliding in the control specimen. Changes in the length of Region II between different groups are due to the variability in the tail length and woven length of the fabric. The measured tail length and woven length varies from 16 to 28 mm and 27 to 36 mm, respectively.

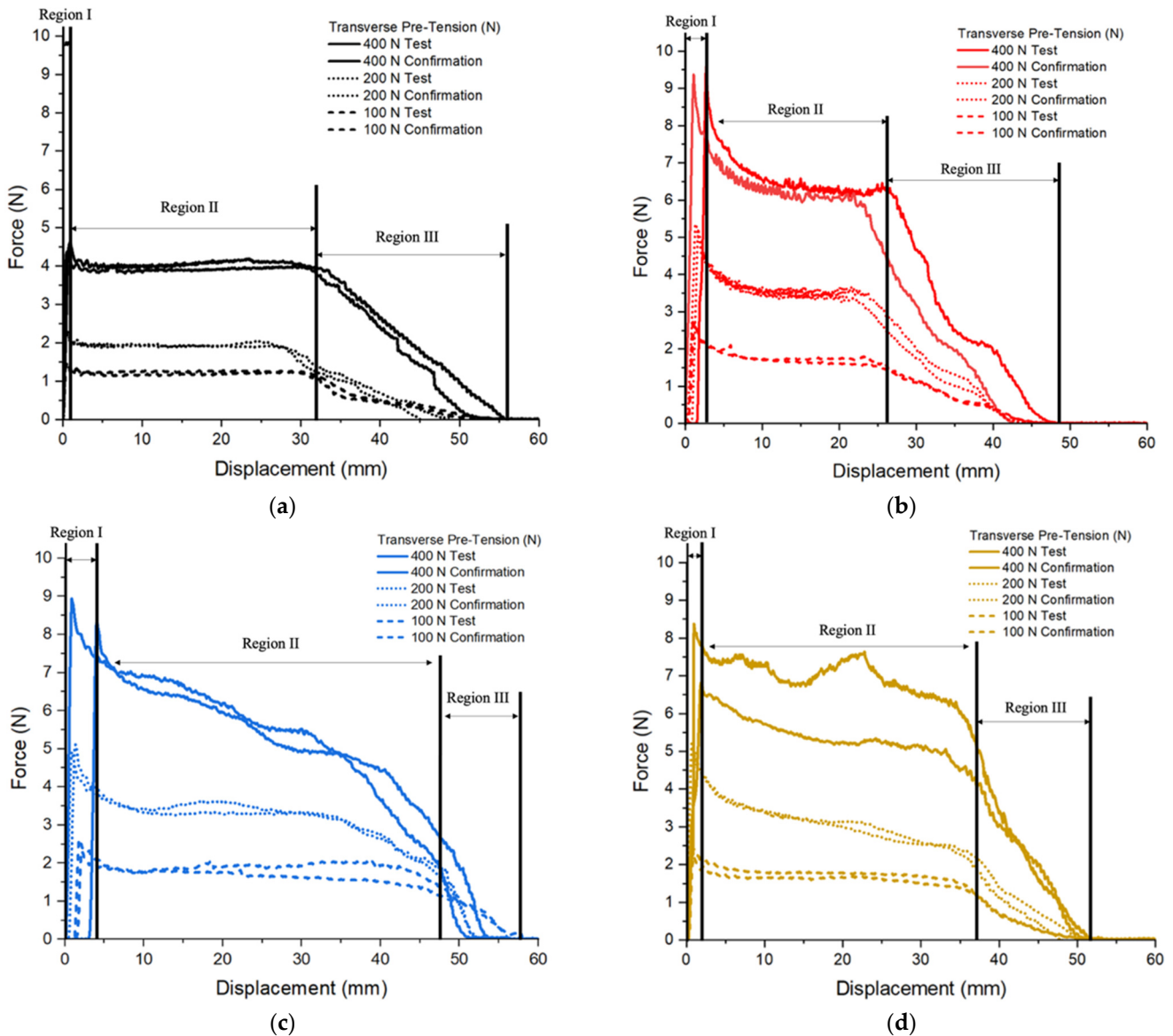


Figure 9. Cont.

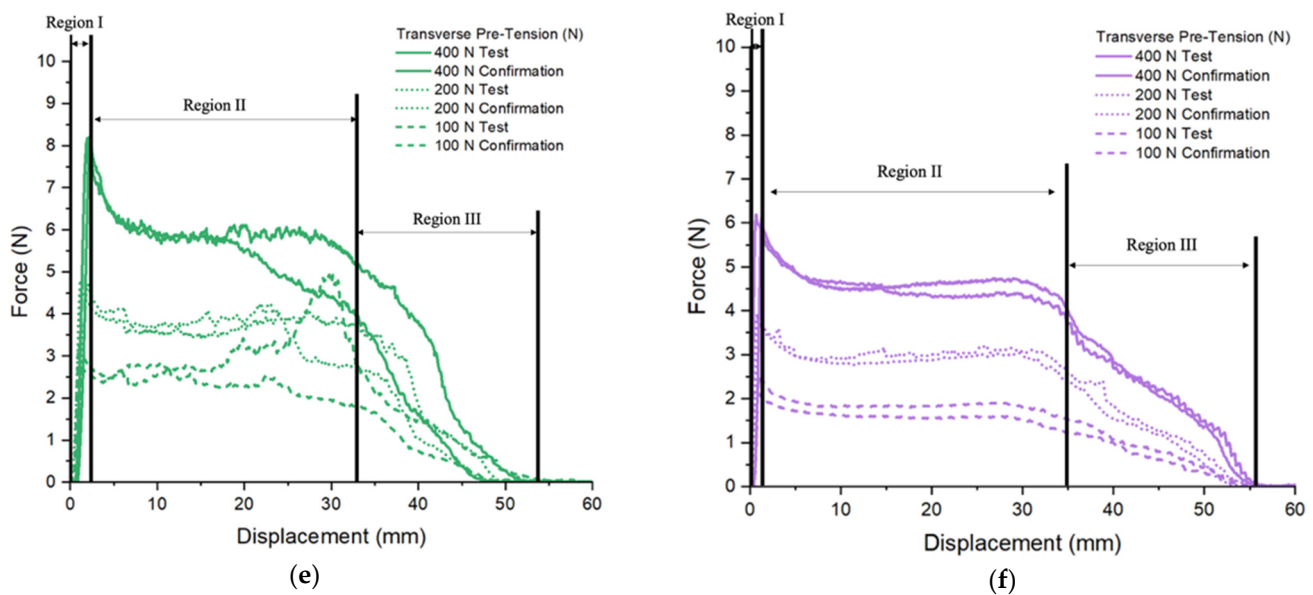


Figure 9. Yarn pull-out force–displacement response of control and metal-coated groups. (a) Control (tail length—20.63 mm; woven length—28.60 mm); (b) Aluminum (tail length—15.82 mm; woven length—31.50 mm); (c) Copper (tail length—28 mm; woven length—27.00 mm); (d) Silver (tail length—22.22 mm; woven length—31.75 mm); (e) Al/AlN (tail length—20.00 mm; woven length—36.00 mm); (f) Hybrid Al/Control (tail length—23.27 mm; woven length—32.50 mm).

Peak pull-out force corresponding to yarn uncrimping and force in Region II corresponding to yarn translation can be used to rank effectiveness of coating for ballistic impact applications. As shown in Figure 10a, peak pull-out force for all the metal-coated groups is higher than the control at all the three transverse pre-tensions studied. The peak pull-out force increases with an increase in transverse pre-tension for all the groups. Furthermore, the rate of increase in the pull-out force with respect to the transverse pre-tension is higher for all the metal-coated specimens than the control. For example, the peak pull-out force increases by a factor of ~ 3.5 for Aluminum compared to an increase of ~ 3 for control, going from 100 N to 400 N. The peak pull-out forces are also normalized with respect to the corresponding control values and shown in Figure 10b. Clearly, all the metal-coated groups exhibit an increase in the peak pull-out force compared to the control. The pull-out force in Region II during yarn translation is shown in Figure 10c at 100 N and 200 N transverse pre-tensions. Similar to the peak pull-out force, all metal-coated groups show an increase in the Region II yarn pull-out translation force during yarn translation after overcoming static friction.

Numerical simulations of experimental ballistic impact onto a single layer Kevlar[®] fabric at 70 m/s with a spherical projectile [25] showed transverse pre-tension in the principal yarn in the range of 100 to 200 N. Since normalized peak pull-out forces show a maxima at 200 N transverse pre-tension (Figure 10b), Figure 11 shows peak pull-out force and normalized peak pull-out force, as a function of different metal coatings, at a transverse pre-tension of 200 N. All the metal-coated groups except the Hybrid show an increase in the peak pull-out force by a factor of ~ 2 compared to the control. The Aluminum-coated specimen shows the highest normalized pull-out force among all the metal-coated groups and has approximately 2.3 times the peak pull-out force compared to control. On the other hand, the Hybrid Al/Control specimen shows the lowest normalized peak pull-out force among all the metal-coated groups and has approximately 1.5 times the peak pull-out force compared to control. As discussed before, since peak pull-out force in Region I is associated with static friction, these results suggest that all the metal-coated groups exhibit a significantly enhanced static frictional resistance (behavior) compared to the control.

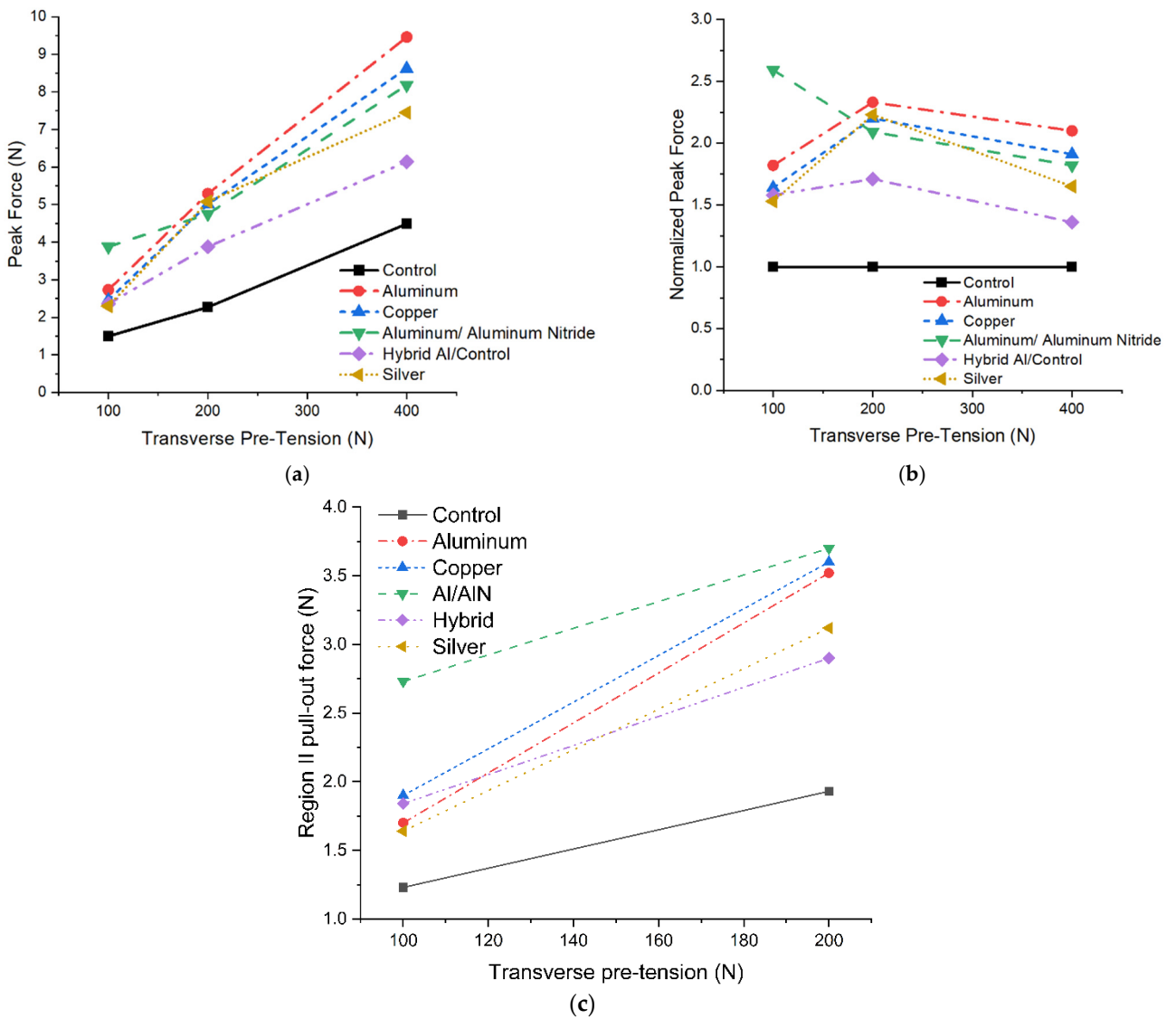


Figure 10. Effect of transverse pre-tension on (a) peak pull-out force (b) normalized peak pull-out force (c) Region II yarn pull-out translation force.

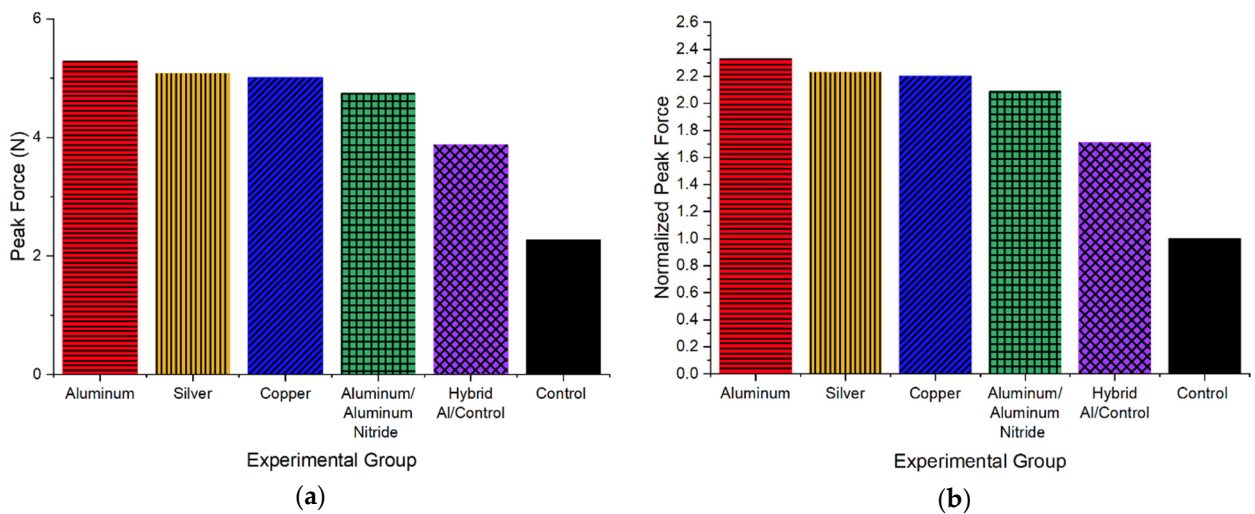


Figure 11. Peak pull-out force at 200 N transverse pre-tension (a) peak force (b) normalized peak pull-out force with respect to control.

Yarn pull-out (yarn uncrimping and yarn translation) mechanism is a major contributor towards ballistic energy absorption [26]. For ballistic resistance, both forces in Region I and Region II, and also the energy absorbed during pull-out including both Regions I (uncrimping) and Region 2 (translation) could be important depending on the number of fabric layers. Therefore, in addition to pull-out force, pull-out energy is useful for ranking effectiveness of coating. The energy absorbed during the pull-out process due to uncrimping and yarn translation at various transverse pre-tensions is shown in Figure 12a. Similar to the peak pull-out force, energy absorbed also increases with increase in transverse pre-tension for all the groups studied. Normalized pull-out energy absorption with respect to the corresponding control values is shown in Figure 12b. All the metal-coated groups exhibit an increase in energy absorption compared to the control.

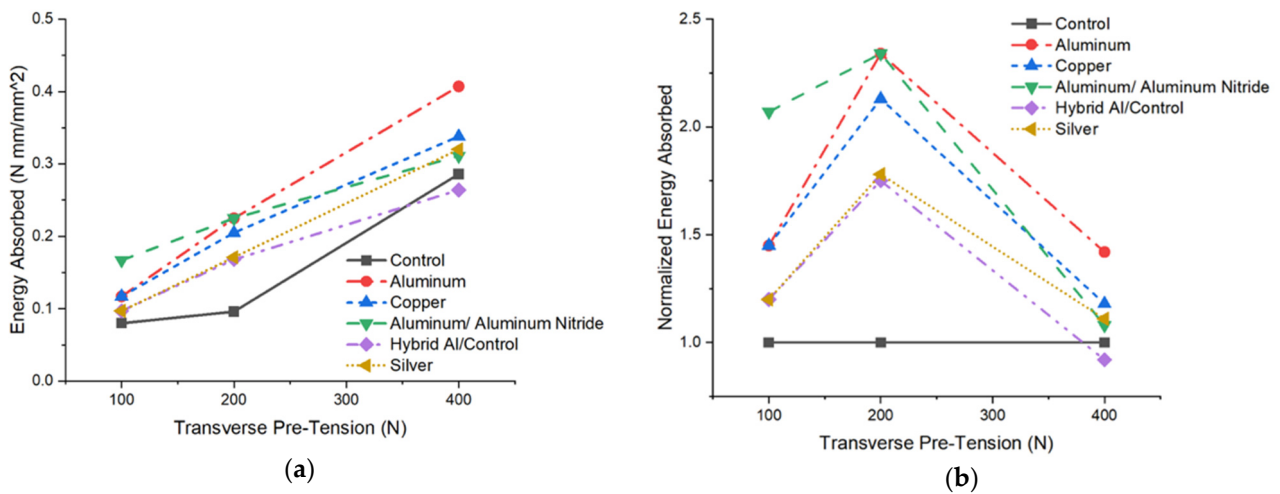


Figure 12. Effect of transverse pre-tension on (a) energy absorbed (b) normalized energy absorbed.

Since normalized energy absorbed shows a maxima at 200 N transverse pre-tension (Figure 12b), Figure 13 shows energy absorbed, and normalized energy absorbed, as a function of different metal coatings, at a transverse pre-tension of 200 N. Aluminum specimen shows the highest increase in energy absorption by a factor of ~2.3 compared to the control. Silver and Hybrid Al/Control shows the lowest energy absorption among the metal-coated groups with an increase of ~1.8 compared to control.

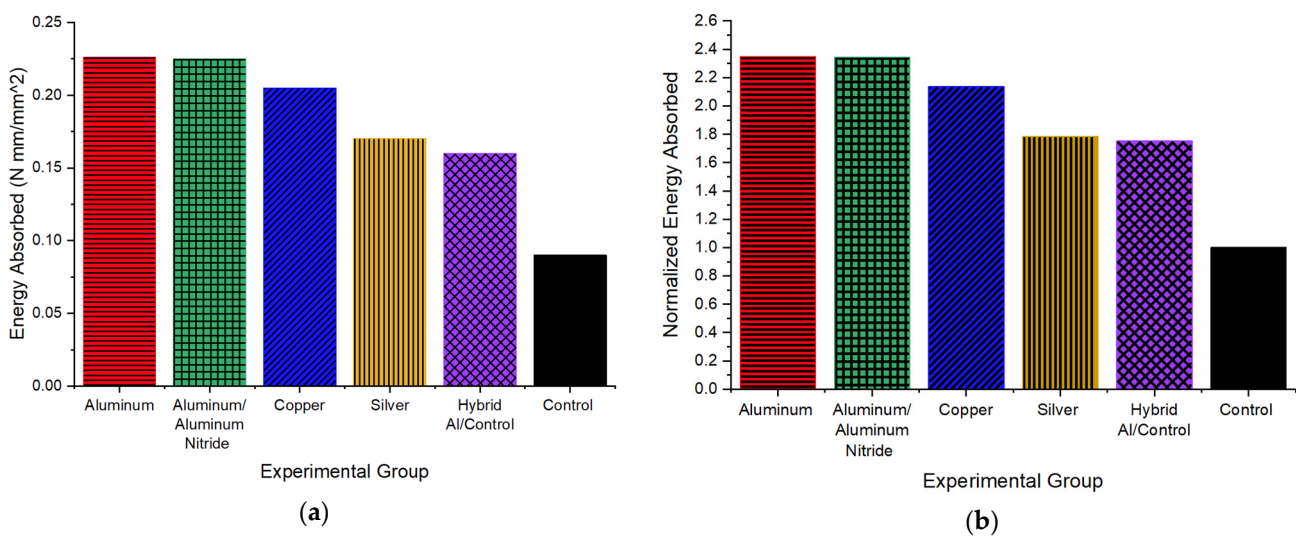


Figure 13. Energy absorbed at 200 N transverse pre-tension (a) energy absorbed (b) normalized energy absorbed with respect to control.

3.2. Inter-Yarn Friction Coefficient Calculations

The peak pull-out force depends on the fabric architecture and the friction coefficient between the warp and weft yarns among other factors. An empirical relation for the pull-out force proposed in [5] is given in Equation (2). Here, F is the normalized yarn pull-out force per unit fabric length, count is the fabric count in yarns per inch, Diameter is the measured fiber diameter in meters, Modulus is the fiber modulus in Pascal, Waviness is the yarn waviness in meters, Friction indicates the coefficient of cross-yarn friction, and C = 0.573 is a constant obtained in [5] from fitting yarn pull-out experimental data without any transverse pre-tension for commercial Kevlar fabrics to Equation (2).

$$F = C \times \text{count}^4 \times \text{Diameter}^2 \times \text{Modulus} \times \text{Waviness} \times \text{Friction} \quad (2)$$

Equation (2) is used to determine the inter-yarn friction coefficients of the hand-woven fabrics studied in this work. It should be noted that this Equation (2) does not consider both the tightness of the weave in the fabric and the effect of transverse pre-tension. Yarn pull-out experiments for the As-received Kevlar® S706 fabric with zero-tail length are first performed without any transverse pre-tension to verify the applicability of Equation (2). Force–displacement response for Kevlar® S706 specimens with a nominal fabric length of 25.4 mm is shown in Figure 14. It should be noted that Region II is absent in Figure 14 due to the zero-tail length. Using the measured normalized peak pull-out force per unit fabric length and other parameters listed in Table 2, a friction coefficient of 0.20 is calculated for the S706 fabric which is comparable to the cross-yarn friction of 0.248 reported in [5] for Kevlar® K706 fabric with KM2 yarns.

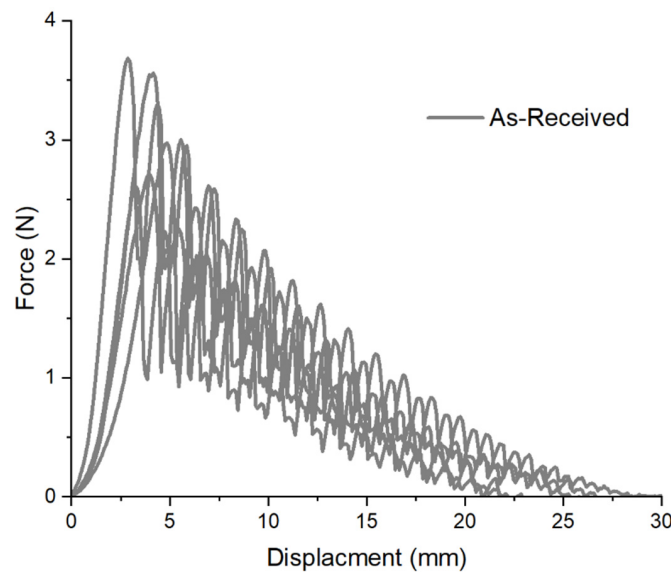


Figure 14. Pull-out response of the As-received Kevlar® S706 fabric with zero-tail length and without any transverse pre-tension.

Table 2. Sample calculations for friction coefficient using Equation (2).

Parameters	Units	As-Received Kevlar® S706 without Any Pre-Tension	As-Received Kevlar® S706 with 100 N Pre-Tension	Hand-Woven Control with 100 N Pre-Tension
F	N/m	2.57/0.0254 = 101.18	6.457/0.032 = 201.79	1.495/0.02858 = 52.3
C	–	0.573	0.573	0.573
Count	Yarns per inch	34	34	50
Diameter	Meter	1.2×10^{-5}	1.2×10^{-5}	1.2×10^{-5}
Modulus	Pascal	9.2×10^{10}	9.2×10^{10}	8.683×10^{10}
Waviness	Meter	5×10^{-5}	5×10^{-5}	5×10^{-5}
Friction		0.20	0.397	0.0233

Since all the hand-woven specimens are tested with non-zero transverse pre-tensions (Figure 9), pull-out force corresponding to 100 N pre-tension is used in all the calculations. Table 2 also lists the parameters used for calculating friction coefficient of hand-woven Control group. A friction coefficient of 0.0233 is calculated for the Control group, which is substantially lower (an order of magnitude) compared to the As-received primarily due to the “looseness” of the weave. Since the hand-woven specimens are not as tightly woven compared to the commercially available Kevlar[®] fabrics, the friction coefficient values are normalized with respect to the Control values. Furthermore, waviness and fabric count are assumed to be the same for all the hand-woven specimens. Therefore, pull-out force is influenced by the fiber diameter, modulus, and friction coefficient. Knowing the measured fiber diameter (from Table 1), measured modulus (discussed later in Table 5), and pull-out force per unit fabric length, friction coefficients are calculated for all the groups. Table 3 shows the normalized friction coefficients calculated for all the hand-woven metal-coated groups at a transverse pre-tension of 100 N and 200 N. All the metal-coated groups show an increase in the normalized friction coefficient compared to the Control. The copper-coated specimen shows the highest normalized friction coefficient of 1.75 and 2.34 among all the metal-coated groups. Silver and Hybrid Al/Control shows the lowest normalized coefficient friction of around 1.30 while Aluminum coating’s friction is at 1.52 and 1.93.

Table 3. Normalized friction coefficients at 100 N and 200 N transverse pre-tension.

Experimental Group	Normalized Frictional Coefficient	
	100 N pre-tension	200 N pre-tension
Control	0.0233/0.0233 = 1	1
Aluminum	0.0355/0.0233 = 1.52	1.93
Copper	0.0407/0.0233 = 1.75	2.34
Silver	0.0291/0.0233 = 1.24	1.81
Al/AlN	0.0329/0.0233 = 1.40	1.54
Hybrid Al/Control	0.029/0.0233 = 1.27	1.37

3.3. Surface Profile Evaluation

While the pull-out process is qualitatively similar during each stage, regardless of the type of coating (Figure 8), frictional coefficients differ between coated and uncoated groups. To better understand these differences, surface profiles of the individual single fibers are studied using a Nanotec WSxM Atomic-Force Microscopy (AFM) in either contact or tapping mode. A small piezo probe with a tip radius of 50 nm is used for imaging As-received and Copper-coated single fibers, whereas a medium piezo probe with a tip radius of 50 nm is used for imaging the Aluminum and Control resulting in different scan areas listed in Table 4. The two AFM probes were of the same type for all the measurements. The small piezo scanner used for the initial measurements is different than that used for the rest. Practically, the small one makes it very hard to get the tip on top of the fiber.

Table 4. Atomic-Force Microscopy (AFM) surface profile evaluation.

	Scan Area (μm^2)	Average Height (nm)	Number of Events	Surface Skewness	Surface Kurtosis
As-Received S706	15.43	23.08	1365	−0.13	3.21
Control	27.41	105.61	1881	−0.31	2.41
Aluminum	27.58	94.577	7500	2.89	25.26
Copper	13.17	25.35	1697	1.74	12.68

Figure 15 shows AFM phase lag images of As-received and metal-coated single fibers with fiber direction indicated by an arrow. That is, phase lag between the drive and response of the cantilever correlated with energy dissipation. Qualitatively, it shows that there is a blob of coating/sizing on the surface running along the fiber direction.

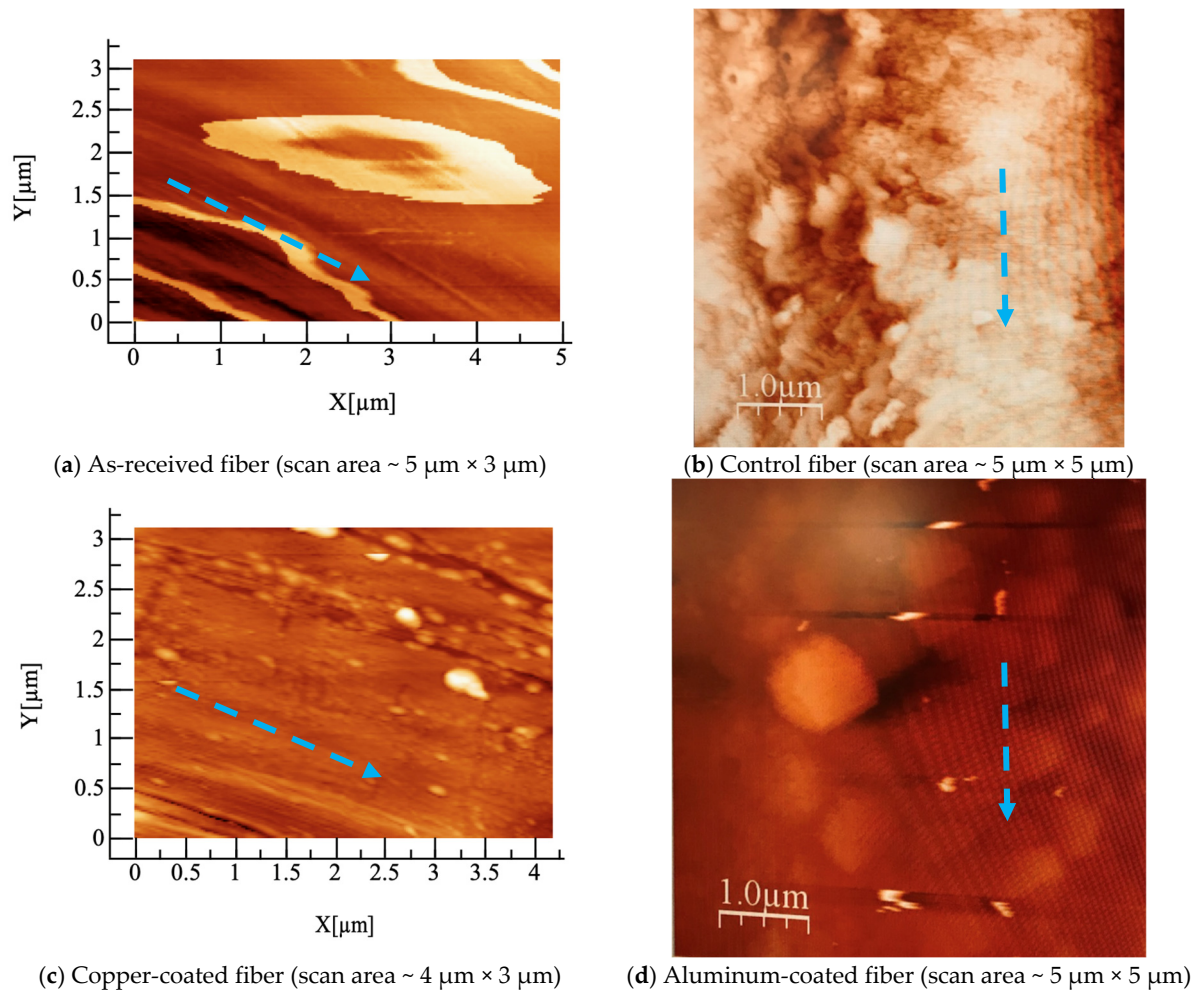


Figure 15. Atomic-Force Microscopy (AFM) images of As-received and metal-coated single fibers with fiber directions indicated by arrows (a) As-received S706 fiber phase image showing variable energy dissipation, presumably due to the sizing (b) Control fiber topography (c) Copper-coated fiber topography (d) Aluminum-coated fiber topography.

Table 4 lists the scanned area and the various surface profile parameters for the fibers studied. Surface skewness indicates whether a profile is biased towards peaks or valleys. A negative skewness value indicates the surface consists of valleys or cracks, and a positive skewness value contains many peaks and asperities. From Table 4, the Control and As-received experimental groups show negative skewness values as well as the lowest coefficient of friction paired with the Hybrid Al/Control experimental group. Surface kurtosis is a measure of sharpness of the profile peaks. A value of 3 for surface kurtosis indicates surface heights are normally distributed. A surface kurtosis value greater than 3 indicates the surface to have an abnormal number of high peaks and valleys whereas. Statistical moment analysis of the surfaces, as summarized in Table 4, show that As-received surfaces have Normal height distributions while metal-coated surfaces are radically non-Normal and fat-tailed (i.e., high Kurtosis), indicating more low and more high points, as would be expected for a roughened surface.

Figure 16 shows a comparison of the surface profile average height distribution for the different fibers. As seen, the aluminum-coated fiber has the largest number of events, nearly 8 times more than the As-received S706 fabric, as well as the largest average height. The increased surface height (roughness) and distribution of the metallic coatings compared to the control is thought to increase the frictional coefficients during pull-out.

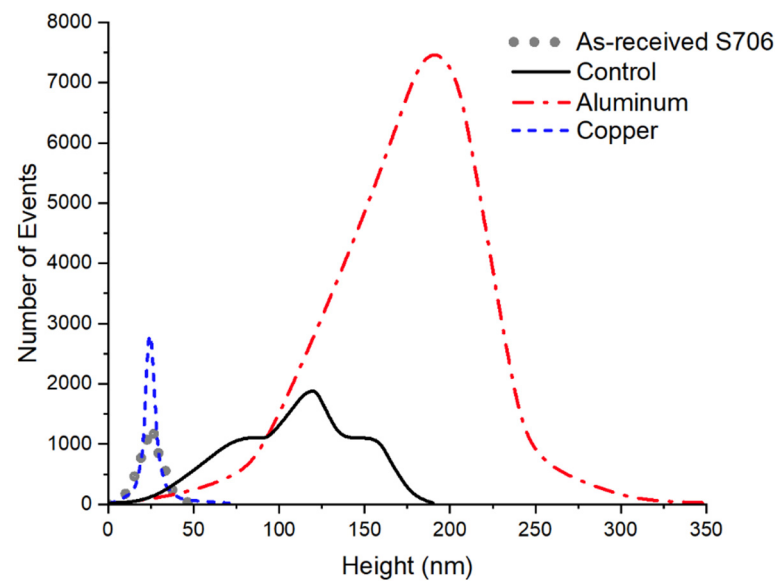


Figure 16. Comparison of surface profile height distribution.

3.4. Tensile Testing Results

Tensile yarn deformation/strength is an important mechanism/property contributing to ballistic performance [19]. The yarn tensile force–displacement measurements are evaluated in terms of tenacity (force per denier) versus strain. Figure 17 shows a comparison of the representative nominal tensile response of all the groups. All the groups exhibited an approximately linear response until reaching the peak force. Upon reaching the peak force, a catastrophic failure of the yarn is observed.

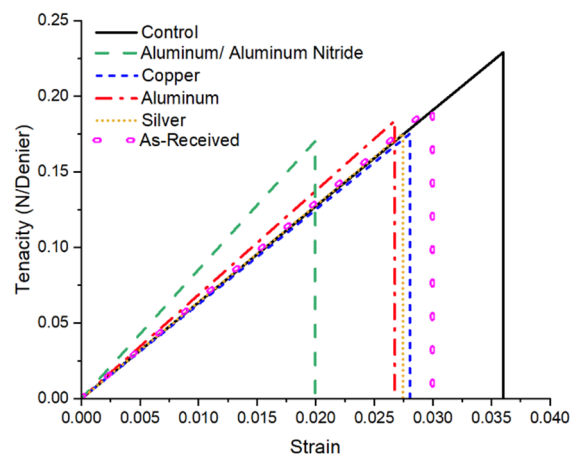


Figure 17. Representative yarn tensile of all groups.

Table 5 lists the tensile modulus and tenacity measurements for all the groups studied. Differences are determined to be statistically significant ($p < 0.05$) by a t-test comparison indicating that the metal-coated groups are significantly different to the control in terms of moduli, tenacity and strain to failure. It should be noted that hot water scouring (i.e., control yarn) resulted in a 4% reduction in the tenacity compared to the yarn directly off the spool. In general, the metal-coated yarns showed a marginal increase in the tensile modulus compared to control. However, the metallic coatings resulted in an average of 21.26% reduction in tenacity for all the metal-coated groups compared to control. This is likely due to damage induced to the fibers by all preparation steps including yarn preconditioning for sizing removal, DVD processing and handling. Further research is needed to better understand the effect of weaving and tenacity reduction mechanisms. Since normalized

peak pull-out force (Figure 10b) and normalized energy absorbed (Figure 12b) show a maxima at 200 N transverse pre-tension, Figure 18 shows the normalized peak pull-out force at 200 N transverse pre-tension versus normalized tenacity. An increase in the peak pull-out force by a factor of ~ 2 (200%) is observed for the metal-coated groups with a decrease in tenacity by $\sim 20\%$ compared to control. Considering the increase in inter-yarn friction coefficients (Table 3) and energy absorbed (Figure 13b) at 200 N pre-tension, and lowest tenacity reduction (Table 5), Aluminum-coated yarns appear to be a suitable candidate for ballistic impact testing.

Table 5. Tensile modulus and tenacity of yarns. Tenacity reduction is calculated relative to the control yarn.

Experimental Group	Modulus (GPa)	True Tenacity (N/Denier)	Relative Tenacity Reduction (%)	Strain to Failure
Control	86.83 ± 2.41	0.229 ± 0.007	-	0.036 ± 0.001
Aluminum	94.01 ± 1.74	0.1834 ± 0.0058	19.91	0.0267 ± 0.0015
Copper	81.33 ± 2.88	0.1749 ± 0.0096	23.62	0.028 ± 0.001
Silver	89.75 ± 3.40	0.1757 ± 0.007	23.27	0.0275 ± 0.0018
Aluminum/Aluminum Nitride	89.11 ± 1.89	0.1706 ± 0.0063	25.50	0.02 ± 0.0007
Hybrid Al/Control	94.01 ± 1.74	0.1834 ± 0.0058	19.91	0.0267 ± 0.0015
As received	92.91 ± 1.19	0.1938 ± 0.007	15.37	0.03 ± 0.0015

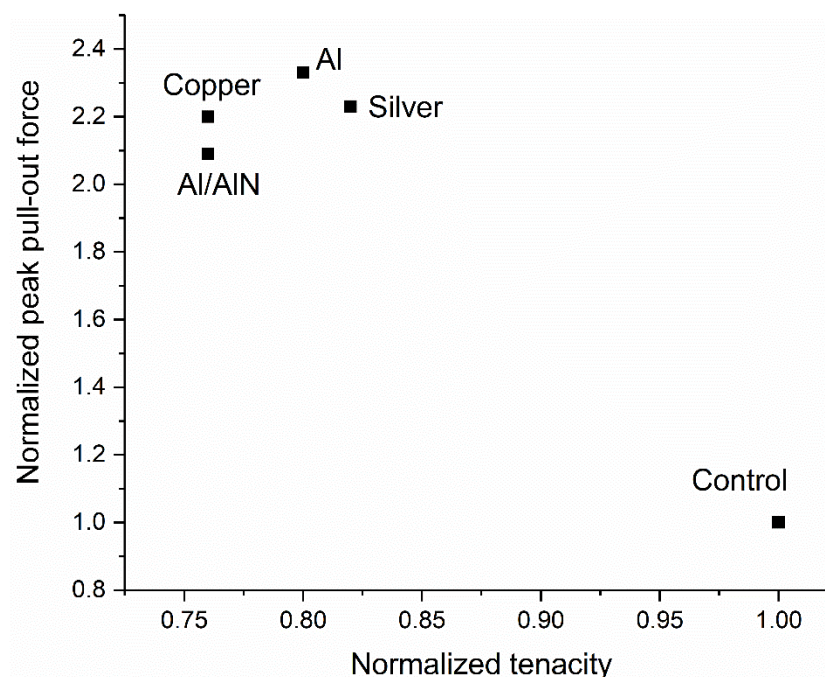


Figure 18. Normalized peak pull-out force at 200 N transverse pre-tension versus tenacity.

4. Conclusions

In this paper, experimental studies on the influence of metallic coating on yarn pull-out behavior in Kevlar[®] fabrics are reported. Kevlar[®] KM2+ individual yarns are coated with metallic layers (copper, aluminum, aluminum nitride and silver) via a directed vapor deposition process. The uncoated control and metal-coated Kevlar[®] yarns are hand-woven into fabric swatches to screen the type of coating for ballistic impact applications. Quasi-static yarn pull-out experiments are performed at three levels of transverse pre-tensions at 100 N, 200 N, and 400 N. Peak pull-out force and pull-out energy absorption due to yarn uncrimping and translation are used to rank the effectiveness of coating for future ballistic

impact testing. Both peak pull-out force and energy absorption during the pull-out process are found to increase with the increase in transverse pre-tension. All the metal-coated groups showed an approximately 200% increase in peak pull-out force and a 20% reduction in tenacity compared to uncoated control. Furthermore, all the metal-coated groups showed an increase in energy absorption, with aluminum-coated yarns showing the highest increase of 230% compared to control. These results suggest enhanced frictional interactions during yarn pull-out in metal-coated yarns compared to uncoated control, indicating its potential for improving ballistic impact performance. However, all the preparation steps including yarn preconditioning for sizing removal, DVD processing and handling resulted in reduced tenacity. Considering the increase in inter-yarn friction coefficients and energy absorbed at 200 N pre-tension, and lowest tenacity reduction, Aluminum-coated yarns appear to be a suitable candidate for ballistic impact testing. The DVD coating process needs further optimization to minimize the reduction in tenacity to enable its use for ballistic impact applications. Future studies include studying the pull-out/ballistic impact response of both tightly woven fabric made of metal-coated yarns versus a tightly woven metal-coated fabric.

Author Contributions: Conceptualization, D.H. and S.S.; methodology, S.S.; formal analysis, J.R., F.D.T. and S.R.C.; investigation, J.R., F.D.T. and S.R.C.; resources, D.J.O. and K.J.S.; data curation, J.R., J.K., D.C. and S.R.C.; writing—original draft preparation, J.R.; writing—review and editing, S.S., F.D.T. and D.H.; supervision, S.S.; project administration, S.S. and D.H.; funding acquisition, S.S. and D.H. All authors have read and agreed to the published version of the manuscript.

Funding: This material is based upon work by the US Army Contracting Command-APG, Natick Contracting Division, Natick, MA under Prime Agreement No. W911QY19C0088 and by Directed Vapor Technologies International, Inc. Any opinions, findings, and conclusions or recommendations expressed in this material are those of the author(s) and do not necessarily reflect the views of the US Army Contracting Command-APG, Natick Contracting Division, Natick, MA or Directed Vapor Technologies International, Inc. Kevlar® As-received S706 fabric used in this work was provided by ARL/Dupont and is gratefully acknowledged.

Data Availability Statement: Not applicable.

Conflicts of Interest: The authors declare no conflict of interest.

References

1. Sockalingam, S.; Chowdhury, S.C.; Gillespie, J.W.; Keefe, M. Recent advances in modeling and experiments of Kevlar ballistic fibrils, fibers, yarns and flexible woven textile fabrics—A review. *Text. Res. J.* **2017**, *87*, 984–1010. [[CrossRef](#)]
2. Sockalingam, S.; Gillespie, J.W.; Keefe, M. Modeling the fiber length-scale response of Kevlar KM2 yarn during transverse impact. *Text. Res. J.* **2017**, *87*, 2242–2254. [[CrossRef](#)]
3. Cunniff, P.M. An analysis of the system effects in woven fabrics under ballistic impact. *Text. Res. J.* **1992**, *62*, 495–509. [[CrossRef](#)]
4. Gawandi, A.; Thostenson, E.T.; Gillespie, J.W., Jr. Tow pullout behavior of polymer-coated Kevlar fabric. *J. Mater. Sci.* **2011**, *46*, 77–89. [[CrossRef](#)]
5. Dong, Z.; Sun, C.T. Testing and modeling of yarn pull-out in plain woven Kevlar fabrics. *Compos. Part A Appl. Sci. Manuf.* **2009**, *40*, 1863–1869. [[CrossRef](#)]
6. Nilakantan, G.; Gillespie, J.W. Yarn pull-out behavior of plain woven Kevlar fabrics: Effect of yarn sizing, pullout rate, and fabric pre-tension. *Compos. Struct.* **2013**, *101*, 215–224. [[CrossRef](#)]
7. Kirkwood, K.M.; Kirkwood, J.E.; Lee, Y.S.; Egres, R.G.; Wagner, N.J.; Eric, D. Yarn pull-out as a mechanism for dissipating impact energy in Kevlar KM-2 fabric Part I: Quasi-static characterization of yarn pull-out. *Text. Res. J.* **2004**, *74*, 920–928. [[CrossRef](#)]
8. Bilisik, K. Properties of yarn pull-out in para-aramid fabric structure and analysis by statistical model. *Compos. Part A Appl. Sci. Manuf.* **2011**, *42*, 1930–1942. [[CrossRef](#)]
9. LaBarre, E.D.; Calderon-Colon, X.; Morris, M.; Tiffany, J.; Wetzel, E.; Merkle, A.; Trexler, M. Effect of a carbon nanotube coating on friction and impact performance of Kevlar. *J. Mater. Sci.* **2015**, *50*, 5431–5442. [[CrossRef](#)]
10. Duan, Y.; Keefe, M.; Bogetti, T.A.; Cheeseman, B.A.; Powers, B. A numerical investigation of the influence of friction on energy absorption by a high-strength fabric subjected to ballistic impact. *Int. J. Impact Eng.* **2006**, *32*, 1299–1312. [[CrossRef](#)]
11. Decker, M.J.; Halbach, C.J.; Nam, C.H.; Wagner, N.J.; Wetzel, E.D. Stab resistance of shear thickening fluid (STF)-treated fabrics. *Compos. Sci. Technol.* **2007**, *67*, 565–578. [[CrossRef](#)]
12. Dong, Z.; Manimala, J.M.; Sun, C.T. Mechanical behavior of silica nanoparticle-impregnated Kevlar fabrics. *J. Mech. Mater. Struct.* **2010**, *5*, 529–548. [[CrossRef](#)]

13. Tan, V.B.C.; Tay, T.E.; Teo, W.K. Strengthening fabric armour with silica colloidal suspensions. *Int. J. Solids Struct.* **2005**, *42*, 1561–1576. [[CrossRef](#)]
14. Groves, J.F.; Mattusch, G.; Morgner, H.; Haas, D.D.; Wadley, H.N. Directed vapour deposition. *Surf. Eng.* **2000**, *16*, 461–464.
15. Buckley, D.H. *Friction and Wear of Tin and Tin Alloys from 110 to 150 °C*; NASA Tech. Note D-8004; National Aeronautics and Space Administration: Washington, DC, USA, 1975.
16. Buckley, D.H. *Friction, Wear, and Lubrication in Vacuum*; National Aeronautics and Space Administration: Washington, DC, USA, 1971.
17. Rabinowicz, E. Friction coefficients of noble metals over a range of loads. *Wear* **1992**, *159*, 89–94. [[CrossRef](#)]
18. Antler, M. Wear and friction of the platinum metals. *Platin. Met. Rev.* **1966**, *10*, 2–8.
19. Sockalingam, S.; Casem, D.; Weerasooriya, T.; McDaniel, P.; Gillespie, J. Experimental Investigation of the High Strain Rate Transverse Compression Behavior of Ballistic Single Fibers. *J. Dyn. Behav. Mater.* **2017**, *3*, 474–484. [[CrossRef](#)]
20. Sockalingam, S.; Gillespie, J.W.; Keefe, M. International Journal of Solids and Structures Dynamic modeling of Kevlar KM2 single fiber subjected to transverse impact. *Int. J. Solids Struct.* **2015**, *67–68*, 297–310. [[CrossRef](#)]
21. Sockalingam, S.; Gillespie, J.W.; Keefe, M. Influence of multiaxial loading on the failure of Kevlar KM2 single fiber. *Text. Res. J.* **2018**, *88*, 483–498. [[CrossRef](#)]
22. Zhu, D.; Soranakom, C.; Mobasher, B.; Rajan, S.D. Experimental study and modeling of single yarn pull-out behavior of kevlar[®] 49 fabric. *Compos. Part A Appl. Sci. Manuf.* **2011**, *42*, 868–879. [[CrossRef](#)]
23. Das, S.; Jagan, S.; Shaw, A.; Pal, A. Determination of inter-yarn friction and its effect on ballistic response of para-aramid woven fabric under low velocity impact. *Compos. Struct.* **2015**, *120*, 129–140. [[CrossRef](#)]
24. *ASTM D7269*; Standard Test Methods for Tensile Testing of Aramid Yarns. ASTM International: West Conshohocken, PA, USA, 2017.
25. Yu, J.H.; Dehmer, P.G.; Yen, C.F. *High-Speed Photogrammetric Analysis on the Ballistic Behavior of Kevlar Fabrics Impacted by Various Projectiles*; Report ARL-TR-5333; Army Research Laboratory: Aberdeen Proving Ground, MD, USA, 2010.
26. Kirkwood, J.E.; Kirkwood, K.M.; Lee, Y.S.; Egres, R.G., Jr.; Wagner, N.J.; Wetzell, E.D. Yarn pull-out as a mechanism for dissipating ballistic impact energy in Kevlar[®] KM-2 fabric: Part II: Predicting ballistic performance. *Text. Res. J.* **2004**, *74*, 939–948. [[CrossRef](#)]

Disclaimer/Publisher's Note: The statements, opinions and data contained in all publications are solely those of the individual author(s) and contributor(s) and not of MDPI and/or the editor(s). MDPI and/or the editor(s) disclaim responsibility for any injury to people or property resulting from any ideas, methods, instructions or products referred to in the content.